Analysis of Yebes 40 m RT subreflector model at Q band

A. Díaz Pulido, A.Moreno Signes, P. de Vicente

Informe Técnico IT-OAN 2015-16

Revision history

Version	Date	Author	Updates
1.0	10-10-2015	A. Díaz-Pulido, A.Moreno Signes, P. de Vicente	First version
2.0	01-12-2015	A. Díaz-Pulido, A.Moreno Signes, P. de Vicente	Second version
3.0	22-01-2016	A. Díaz-Pulido, A.Moreno Signes, P. de Vicente	Third version

Contents

1 Introduction

On May 27th 2015, while performing an astigmatism measurement of the main reflector (M1) of the 40 m antenna at Q band (43 GHz), several pointing scans where done axially defocusing the sub-reflector (M2). We discovered some systematic pointing errors dependent on the focus position. These errors are caused by an anomalous behaviour of the 6 linear drives of the sub-reflector as already described by [de Vicente (2010)]. This effect is as if the subreflector tilted while moving it along the Z axis.

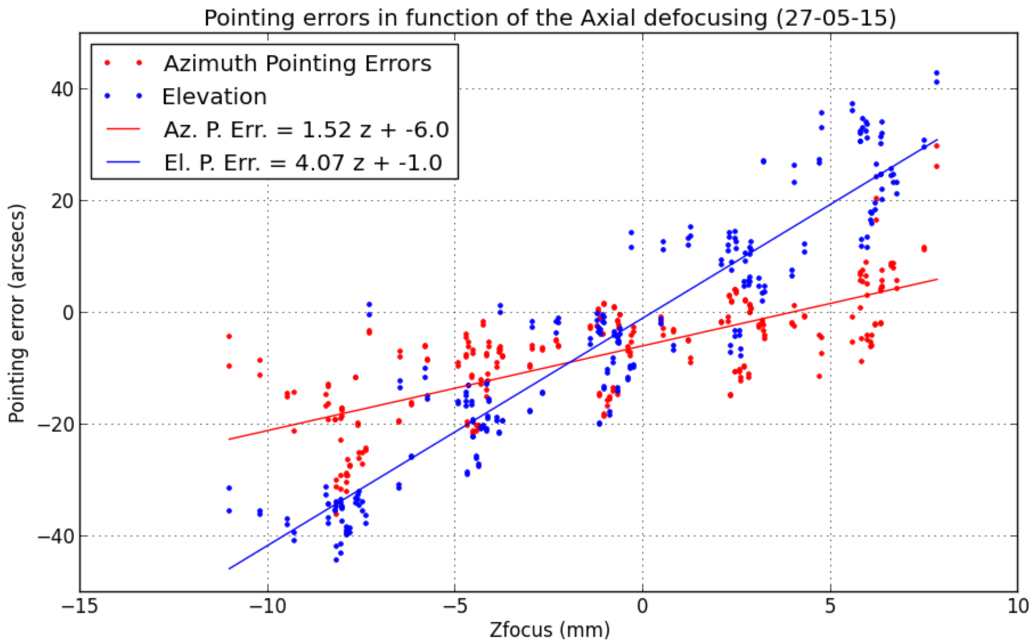

Figure 1: *Pointing errors caused by axial defocusing, possibly due to a tilted sub-reflector.*

In order to investigate these and other possible errors due to the sub-reflector movement, we performed a series of observations to check the parameters currently implemented in the sub-reflector model (elevation dependent). In this report we summarize the observations performed and the results obtained.

2 Pointing shift due to Z focusing

As mentioned in the introduction, de Vicente (2010) found systematic pointing errors when axially defocusing the sub-reflector. To correct for these errors a modification in the model of the subreflector position as function of elevation was implemented. This modification consisted in applying a sub-reflector tilt according to equations 1 and 2. However these parameters, determined with the 22 GHz receiver mounted in M4' branch, seem to have changed (the 45 GHz receiver is currently in M4 branch) and we have reviewed them.

$$\Delta\theta_x = +9.8\,\Delta z \tag{1}$$
$$\Delta\theta_y = -1.2\,\Delta z \tag{2}$$

where δz is in mm and $\Delta\theta_x$ (tilt around the X axis) and $\Delta\theta_y$ (tilt around the Y axis) are in arcseconds.

We have determined the current equivalence between sub-reflector tilt and pointing errors: a tilt around the X axis causes a pointing error in elevation and a tilt around the Y axis causes a pointing error in azimuth. We performed some pointing drifts with different sub-reflector tilts. In all cases during the observations the sub-reflector position was fixed to avoid errors from the anomalous movement. The results from these observations are displayed in Fig. 2.

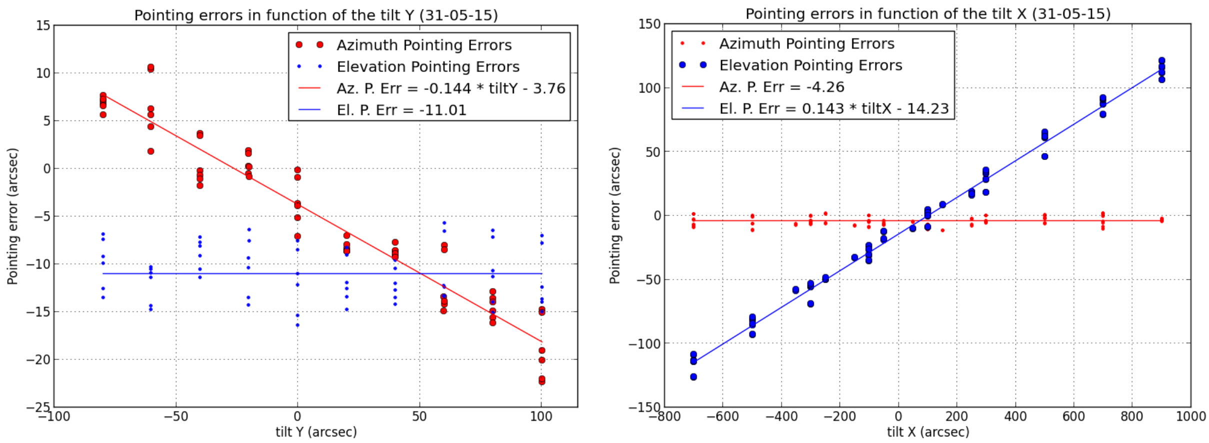

Figure 2: *Pointing errors caused by a tilt in the sub-reflector.*

As expected, a tilt around X has no effect on the azimuth pointing errors and a tilt around Y causes no elevation pointing errors. We performed linear least squares fits to the data as shown in Fig. 2. The dependency is given by:

$$\Delta El = +0.143\,\Delta\theta_x - 14.23 \tag{3}$$
$$\Delta Az = -0.144\,\Delta\theta_y - 03.76 \tag{4}$$

where the tilt and the pointing errors are in arcseconds.

The dependency is mainly given by the slope of the lines. The offset can be absorbed in P2 and P7 parameters of our pointing model (de Vicente 2007). The 0.144 value of the slope matches the theoretical value mentioned by de Vicente (2010) and computed by Barcia (1995). The determination of the slope for the tilt around Y is less reliable than for the tilt around the X axis since the range is much shorter in the former than in the latter. Months later these parameters were checked again (see appendix A), giving almost the same values:

$$\Delta El = +0.143\,\Delta\theta_x \tag{5}$$
$$\Delta Az = -0.146\,\Delta\theta_y \tag{6}$$

Once we obtained the relation between the sub-reflector tilt and the pointing errors we just needed to meassure the pointing errors caused by an axial defocusing. As with the astigmatism observations, we performed pointing drifts with different positions of the sub-reflector along the Z axis and obtained different pointing errors for each set of data (see left panels of Fig. 3). The right panels of Fig. 3 show the tilts around the X and Y axes versus the axial sub-reflector position, once we divided the pointing errors by the slope in 3 and 4 equations. That is, we assumed the pointing errors were caused by tilts in the subreflector. Finally we least square fitted each set obtaining the required tilts to have no pointing errors compensating the sub-reflector movement in the Z axis.

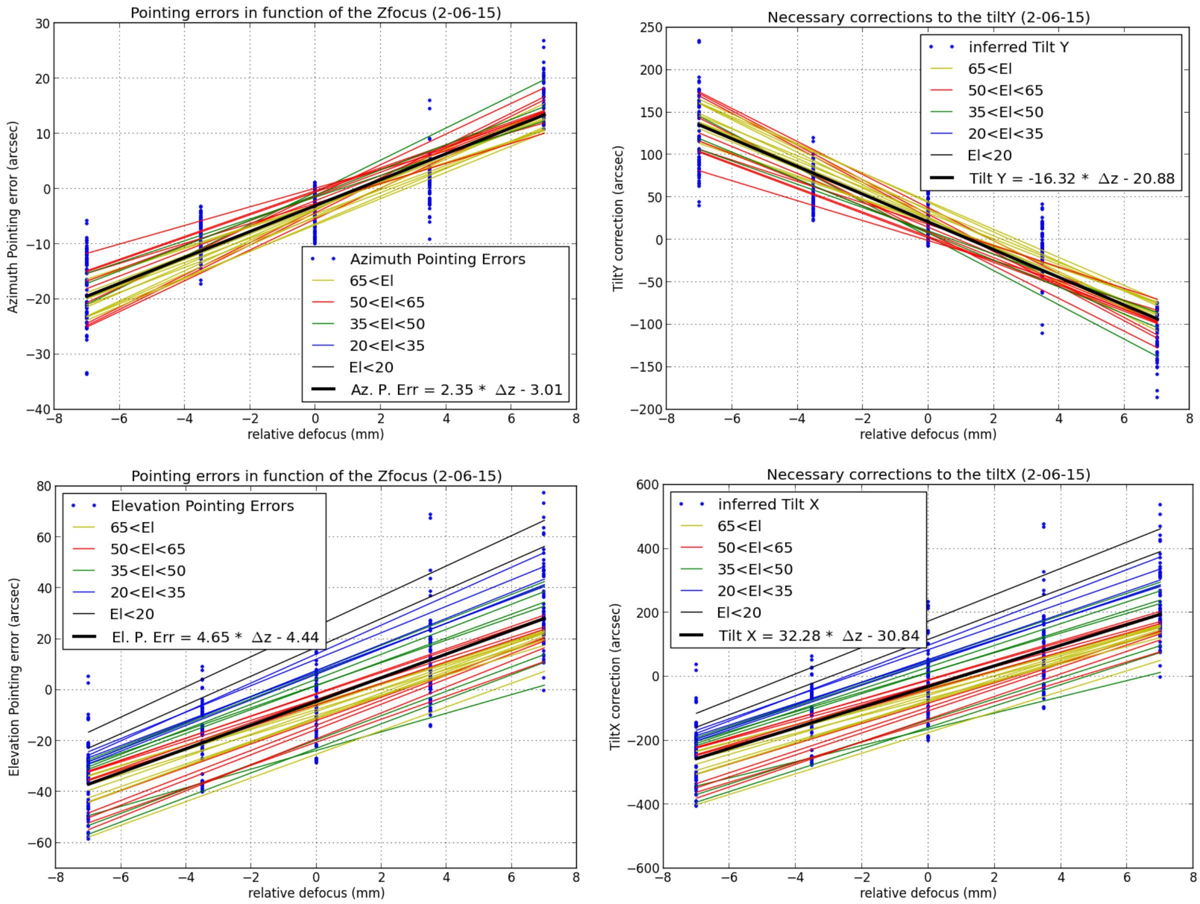

Figure 3: *Left: pointing errors caused by an axial defocus. Right: tilt equivalence for the pointing errors.*

We have obtained an average from the different data sets (done at different elevations). The tilts are:

$$\Delta\theta_x = +32.28\,\Delta z - 30.84 \tag{7}$$

$$\Delta\theta_y = -16.32\,\Delta z - 20.88 \tag{8}$$

where Δz is in mm and the tilts in arcseconds.

The previous results were obtained while the current model, the one given by equations 1 and 2, was active, therefore the obtained parameters are relative to the current ones. After taking it into account, the final model, only taking into account the slopes, is given by

$$\Delta\theta_x = -22.47\,\Delta z \tag{9}$$
$$\Delta\theta_y = +15.12\,\Delta z \tag{10}$$

The new model differs largely from the old one. Currently (see Fig. 3) a shift in the subreflector along the Z axis causes a pointing error of $2.5''$ in azimuth and $4.6''$ in elevation, numbers which can be large at high observing frequencies.

3 X/Y Tilt corrections versus Y/X focus position

It is well known that a movement of the sub-reflector along its X or Y axis causes a pointing error in azimuth or elevation respectively. The 40 m line command utility takes this effect into account and may, if specified, correct the pointing accordingly. The linear dependence is:

$$\Delta Az = +11\,\Delta x \tag{11}$$
$$\Delta El = +11\,\Delta y \tag{12}$$

where the lateral displacements are expressed in mm and the pointing errors in arcseconds.

However we believe that the best option to prevent a pointing error when moving the sub-reflector laterally is to tilt it. We have investigated the ammount of tilt required by doing some observations which consisted on making tilt drifts for different X and Y fixed positions and looking for those which had no pointing error. Shifts along the X axis were compensated with a tilt around the Y axis and shifts along the Y axis with a tilt around the X axis. The best tilt positions around Y and around X as a function of X and Y respectively are shown in Fig. 4.

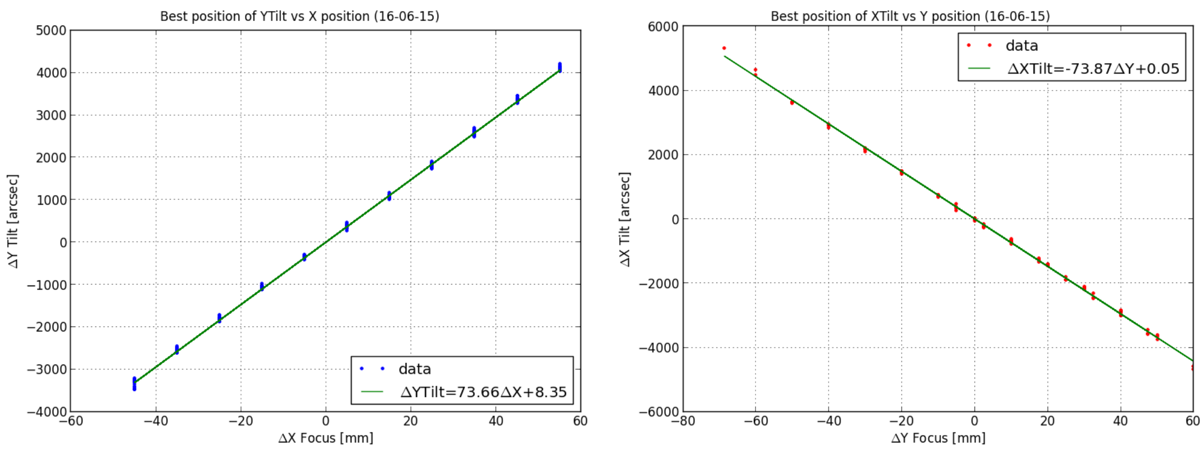

Figure 4: *Left: Best tilt around Y versus X shift. Right: Best tilt iaround X versus Y shift.*

The dependency is linear and the slope obtained is approximately the same for both axis, although the sign is opposite. The difference in sign comes from the way angles are measured for tilts around the Y axis, but in both cases the sub-reflector is tilted towards the vertex to compensate for the lateral shift.

$$\Delta\theta_y = +73.66\,\Delta x \tag{13}$$
$$\Delta\theta_x = -73.87\,\Delta y \tag{14}$$

We have implemented the average of both values for both axes in the code.

Using the relationship between the tilts and the pointing errors given by 3 and 4 we have estimated (again) the relation between the lateral subreflector shifts and the pointing errors. We obtain:

$$\Delta Az = +10.6\,\Delta x \tag{15}$$
$$\Delta El = +10.6\,\Delta y \tag{16}$$

which are very similar to the dependence we already determined in 11 and 12

In the current 40 m line command utility we have added an option to compensate a shift of the subreflector along the X or Y axis either by a manual pointing correction or by tilting the subreflector. We have used equations 11, 12 for pointing corrections and 13 and 14 for corrections which require a tilt.

4 New focus function: `generalfocus()`

In order to investigate further the behaviour of the sub-reflector and to search for its optimum position as a function of elevation, we implemented a special method which allowed us to move the subreflector freely. `generalfocus()` is a new function implemented at the 40 m line command utility that allows to define an initial and a final position for the 5 axes: X, Y, Z and tilts around X and Y. The software makes a linear interpolation between both positions and moves the subreflector during the scan between the start and the end position. The goal is to look for the optimum position in any of the axes and compensate the pointing errors with subreflector movements so that these pointing errors do not hamper this search.

4.1 Axial defocus

A typical axial focus scan consists in shifting the sub-reflector along the Z axis while tracking a source. Fig. 5 shows the result of such observation.

According to Baars (2007), the normalized gain for an uniform illumination is given by:

$$g(\beta) = [\frac{\sin(\beta/2)}{\beta/2}]^2 \tag{17}$$

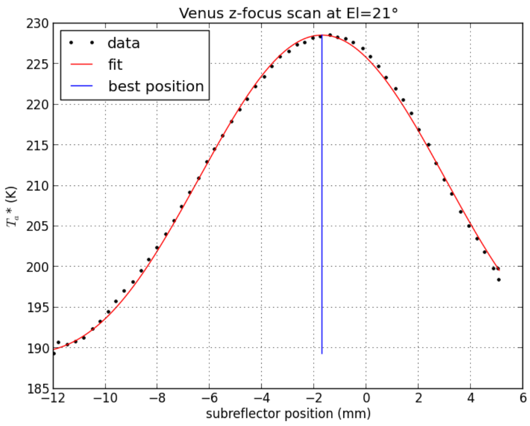

Figure 5: *Axial defocusing scan, using Venus at an elevation of 21 degrees. The abscissa axis scale is relative to the current implemented Z model*

where $\beta = \frac{2\pi\delta}{\lambda}(1 - cos\Psi_0)$, with δ the defocusing, λ the wavelength and Ψ_0 the subtended angle from the focus to the edge of the parabola over the optical axis.

We have performed axial focus observations at different elevations and fitted a function as described in equation 17. Observations were done at night or during the day avoiding moments of high solar radiation that could hamper results by causing deformations in the tetrapod legs. Results are shown in Fig. 6.

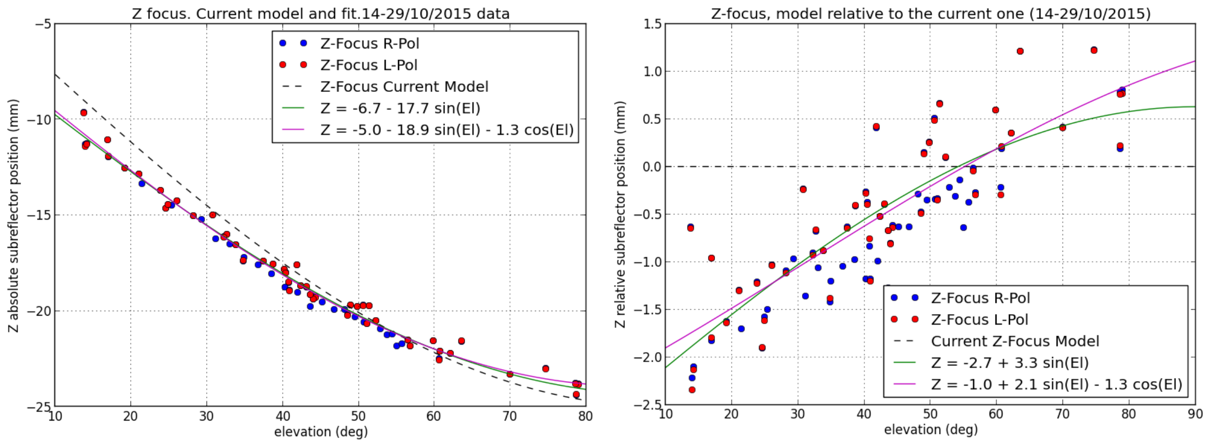

Figure 6: *Best Z position for each telescope elevation. Left panel: absolute positions. Right panel: relative ones to the current model*

The best fit function is a sine type. In the left panel of Fig. 6 we show the current model and the new one using two functions: a sine and a linear combination of sine and cosine. The latter does not provide any significant improvement with respect to the first one. Therefore we have chosen the following dependency as the best one:

$$Z = -6.7 - 17.7\sin(el) \tag{18}$$

Fig. 6 right panel shows the dependence of Z as a function of elevation relative to the current model. Corrections are below $\pm$ 2 mm.

4.2 Lateral defocus

According to a previous section, a lateral shift of the sub-reflector causes a pointing error which can be removed by tilting it. If the correction is not taken into account, as with the `focus()` method the obtained gain curve is thiner (see right panel of Fig. 7). The decrease of signal is steeper because the departure from the optimum position is amplified by the pointing error. If the shift is compensated by the tilt, as with `generalfocus()`, the gain curve is broader and the decrease of power only comes from defocusing (see left panel of Fig. 7).

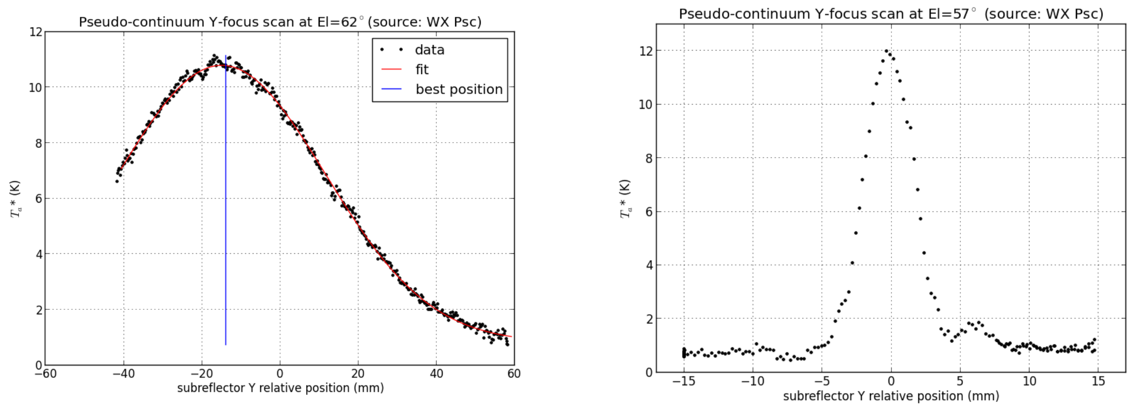

Figure 7: *Lateral focus scan using: $general focus$ function (Left) & $focus$ function (Right). Measures were done at different epochs, hence the difference at the peak intensity*

Therefore `generalfocus()` provides an excellent way to look for the best subreflector lateral position as a function of the telescope elevation.

4.2.1 X-focus model

We have used *generalfocus()* for the lateral focus and tilted the sub-reflector to compensate. A new model of the X-focus has been obtained by fitting curves using equation 17). The results are shown in Fig. 8.

According to appendix C, the subreflector best position for the X-axis should not vary with elevation and therefore we determined a single value by averaging all measurements. The best position found is:

$$X = -17 \tag{19}$$

which will be used for the final sub-reflector model.

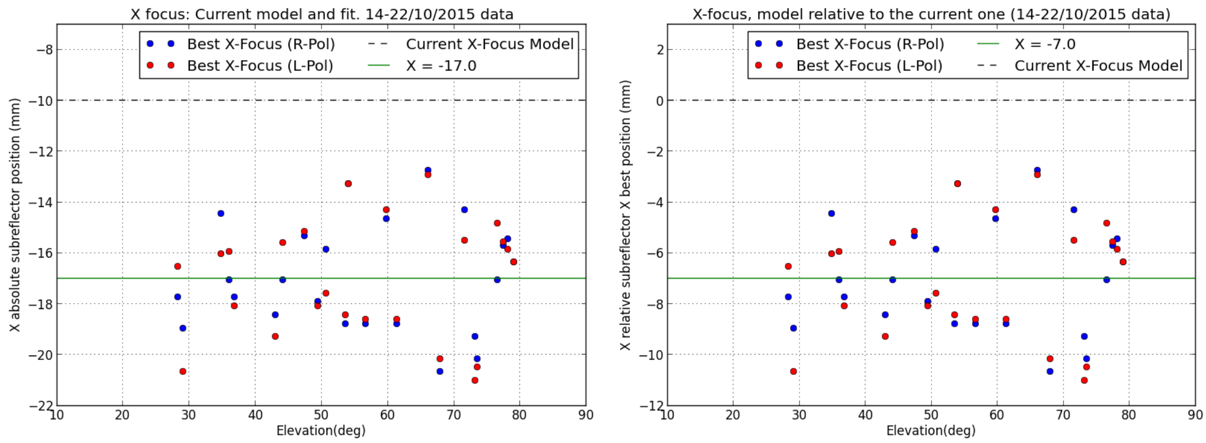

Figure 8: *Lateral X-focus model. Left: absolute position. Right: relative positions*

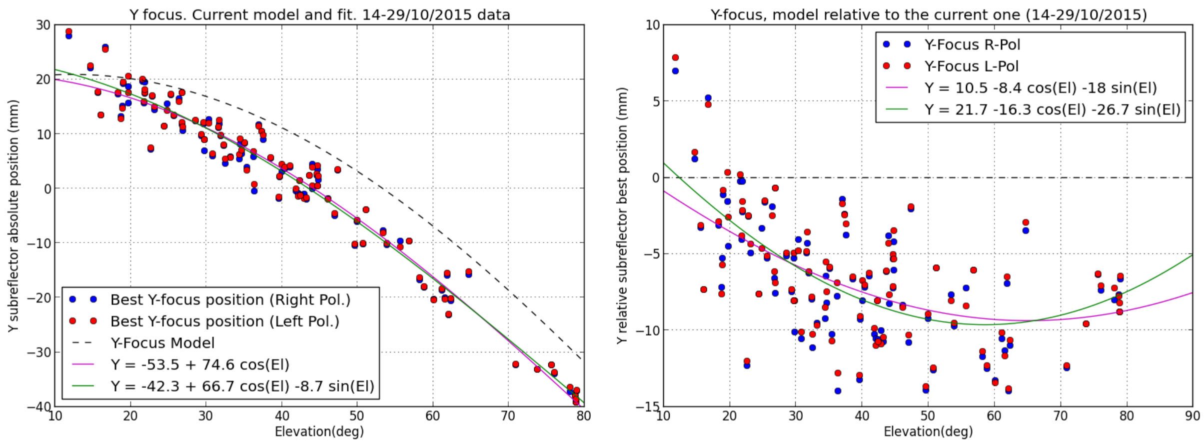

Figure 9: *Lateral Y-focus model. Left: absolute position. Right: relative position to the current model*

4.2.2 Y-focus model

As with the previous case the best position of the subreflector for the Y-axis is shown on figure 9.

We tried two different fits: using a *cosine* function (appendix C) and using a linear combination of *sine* and *cosine*. The latter seems to work better and it is given by:

$$Y = -42.3 + 66.7\,\cos(el) - 8.7\,\sin(el) \tag{20}$$

where Y is in mm, the terms are in arcsecs and el is the elevation.

5 Searching for the optimum tilt of the subreflector

The only dependence of the sub-reflector tilt as a function of elevation included in the model up to now was the one that comes out from equations 18 and 9 and 10. So we were assuming that the tilt was correct and these dependencies came from the anomalous sub-reflector behaviour along the axial axis. However we wanted to know if there is an offset in both tilt positions.

In principle, to obtain the best tilt position, one should track a source while continuously tilting the subreflector. To compensate the pointing error a lateral shift or a continuous pointing correction should be applied along the scan. Both options are not implemened in the control system and would create some uncertainties. A slower but more trustable procedure consists in making some pointing scans with different tilt positions. Each scan requires a pointing correction according to equations 3 and 4. iThe only requirement is that these scans have to be completed quickly to ensure that the elevation and the weather conditions do not change much. The results, obtained fitting a gasussian to the drifts, are shown in Fig. 10. This figure shows the order of magnitude of the tilt required to cause a clear decrease in the detected power; tilts ishould be larger than 1000 arcsecs.

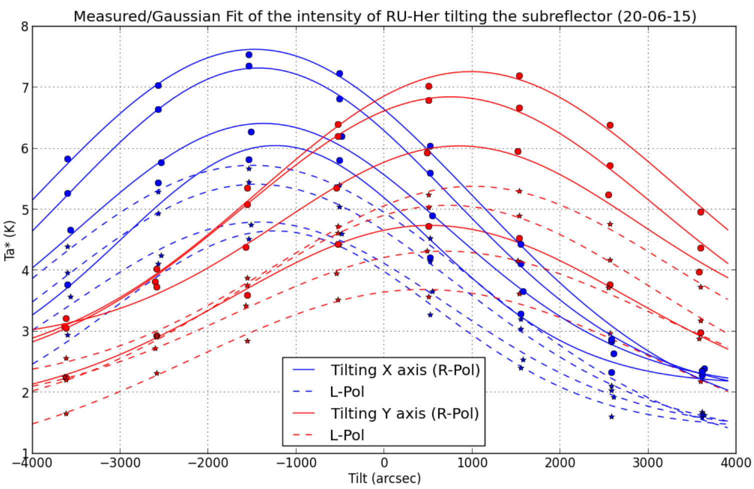

Figure 10: *The effect of an offset in tilt*

5.1 Tilt around Y

We have tried to determine the optimum position for the tilt around Y making pseudocontinuum pointing scans towards three sources with intense maser emission (OriIrc2, R Cas and R Leo). Results are shown at Fig. 11. This test was performed with the old sub-reflector model.

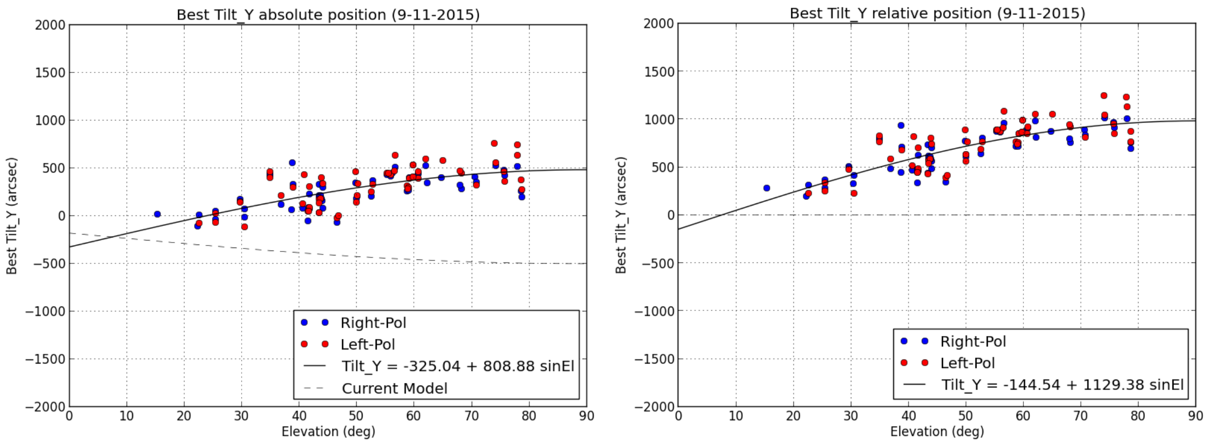

Figure 11: *Best position for the tilt around Y as a function of elevation. Left panel: absolute. Right panel: relative to the model used*

According to Fig. 11 the tilt shows a slight dependence with elevation which has no physical sense. We believe this might be caused by an incorrect operation of the hexapod algorithm.

Since these observations were performed with a position of the subreflector in the X axis of -10 mm and the new model requires a position of -17 mm we have applied a correction to the fitted curve. A shift of -7 mm along the X axis is, according to 13, equivalent to a tilt of $-515''$, which should be added to the fitted curve. The tilt around Y as a function of elevation is then:

$$\theta_y = -515 - 325 + 809 \sin el = -830 + 809 \sin el \tag{21}$$

where the tilt is in arcseconds. This equation was checked later, see appendix B.

5.2 Tilt around X

The tilt around X was determined using the new sub-reflector model for X, Y and Z. As in the previous section, pseudo continuum pointing scans were performed with different tilts around the X axis. The results are shown in Fig. 12.

The dependence of the tilt around X as a function of elevation is:

$$\theta_x = 121 + 1032 \sin el \tag{22}$$

Both functions already contain the dependency of the tilt angles due to the anomalous behaviour of the subreflector when it is moved along the Z axis. Left panels in Figs. 11 and 12 show the contribution from this "anomalous behaviour"as a dotted line.

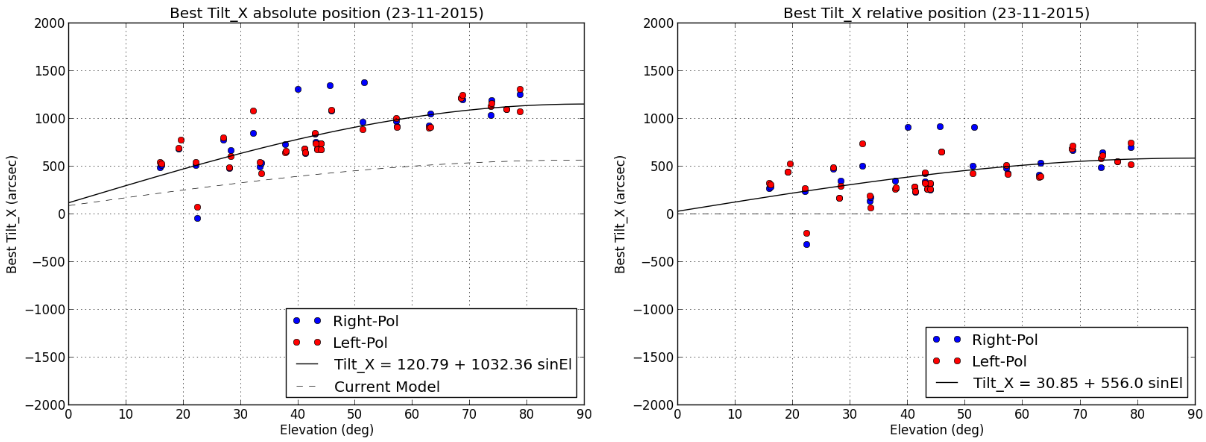

Figure 12: *Best position for the tilt around X as a function of telescope elevation. Left panel: absolute. Right panel: relative to the model used*

6 Final subreflector model

As a result of the discussion showed in previous sections a new subreflector model was implemented the last week of November 2015. Immediately after the implementation of the model a pointing session at 45 GHz plus a gain session was performed to check for changes. Table 6 summarizes the parameters of the new model. Figure 13 shows the aperture efficiency before and after the changes in the models with an improvement around 5%.

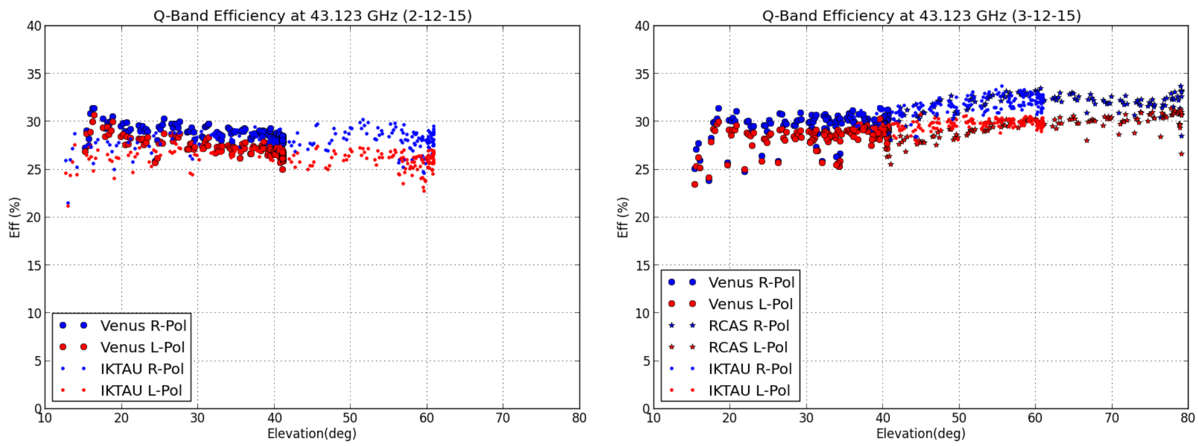

Figure 13: *Aperture efficiency at Q band. Left panel: Old model. Right panel: New model.*

<table>
<tr><td></td><td>Before (May 2015)</td><td>After (December 2015)</td></tr>
<tr><td>Subreflector Model</td><td>x = - 10
y = - 64 + 83 cos El + 18 sin El
z = - 4 - 21.2 sin El
tilt Y = - 39.2 - 207.8 sin El
tilt X = 4.8 + 24.7 sin El</td><td>x = - 17
y = - 42.3 + 66.7 cos El - 8.7 sin El
z = - 6.7 - 17.7 sin El
tilt Y = 3236 -3281 sin El -2895cos El
tilt X = -1524 + 2615 sin El +769cos El</td></tr>
<tr><td>Focus Corrections</td><td>ΔtiltX = + 9.8 Δz
ΔtiltY = - 1.2 Δz
ΔAz = - 0.154 ΔtiltY
ΔEl = + 0.154 ΔtiltX

-
-

ΔAz = 11.0 Δx
ΔEl = 11.0 Δy</td><td>ΔtiltX = - 22.47 Δz
ΔtiltY = + 15.12 Δz
ΔAz = - 0.146 ΔtiltY
ΔEl = + 0.143 ΔtiltX

ΔtiltY = + 73.8 Δx
ΔtiltX = - 73.8 Δy
or
ΔAz = 10.6 Δx
ΔEl = 10.6 Δy</td></tr>
<tr><td>Pointing Model</td><td>P1 = 2522
P2 = 47
P3 = 60
P4 = 10
P5 = 10
P6 = 0
P7 = -1052
P8 = 211
P9 = 854</td><td>P1 = 2925
P2 = -489
P3 = 529
P4 = 12
P5 = 8
P6 = 0
P7 = -1072
P8 = 367
P9 = 810</td></tr>
</table>

References

[de Vicente (2010)] P. de Vicente, *Is the subreflector of the 40 m radiotelescope tilted?*, IT-OAN 2010-15

[de Vicente and Barcia (2007)] P. de Vicente, A. Barcia, *Deconstructing a pointing model for the 40M OAN radiotelescope*, IT-OAN 2007-26

[Barcia (1995)] A. Barcia, *Efectos de las deformaciones de la geometría sobre la puntería de la antena ESSCO de 45 pies*, IT-CAY 1995-8

[Baars (2007)] J. Baars, *The paraboloidal reflector antenna in radio astronomy and communication*, 2007

A Pointing errors VS tilt checking

After implementing equations: $\Delta El = +0.144\ \Delta TX$ and $\Delta Az = -0.144\ \Delta TY$, on the software control database, to avoid pointing errors when the subreflector is tilted, we can see on Fig. 14 that is needed to modify these laws by adding the value of each slope.

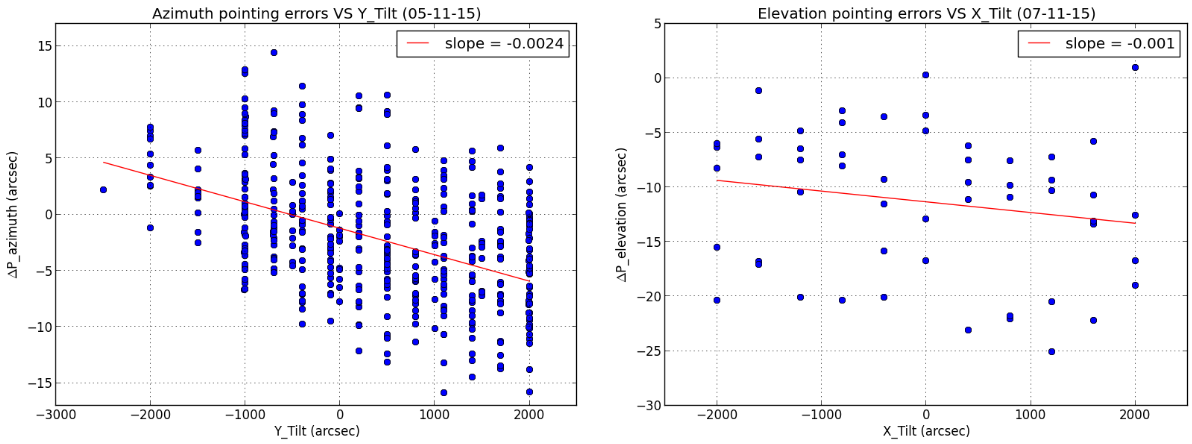

Figure 14: *Pointing errors caused by a tilt at the sub-reflector.*

B Subreflector model checking

In order to make sure that the subreflector model was fine it was done a test. Lateral defocus model was alright, also tilt-X model, but the tilt-Y model required some corrections as can be appreciated in figure 15.

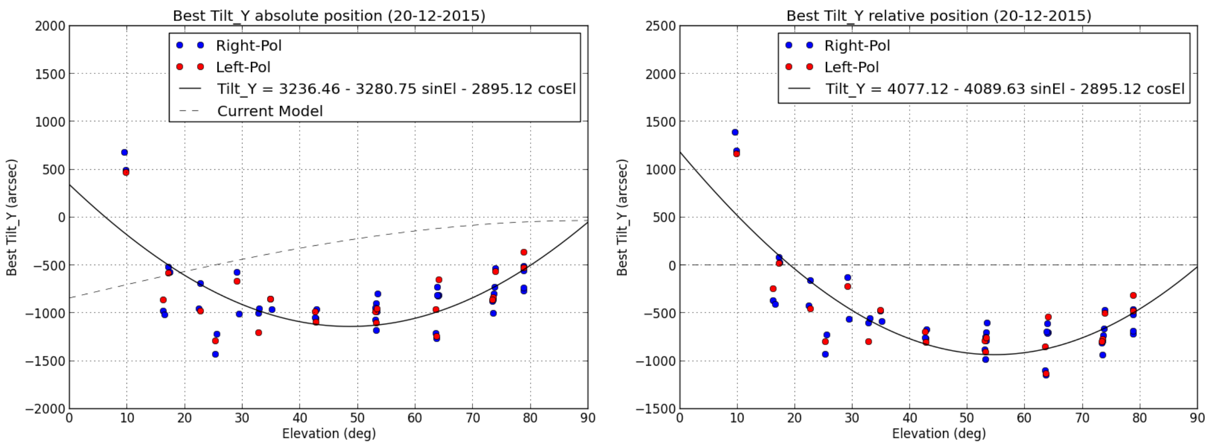

Figure 15: *Best position for the tilt around Y as a function of elevation. Left panel: absolute. Right panel: relative to the model used*

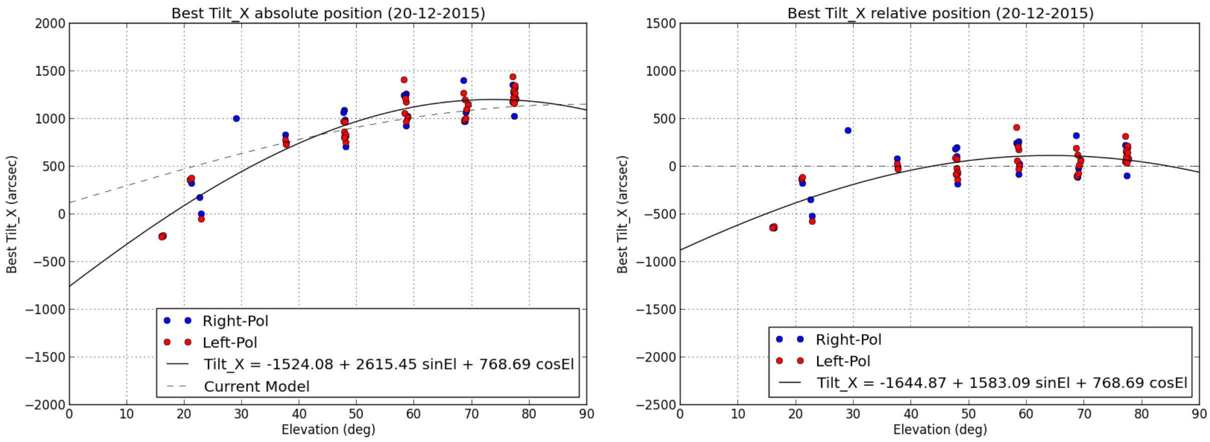

Figure 16: *Best position for the tilt around X as a function of elevation. Left panel: absolute. Right panel: relative to the model used*

C Theoretical gravity deformations

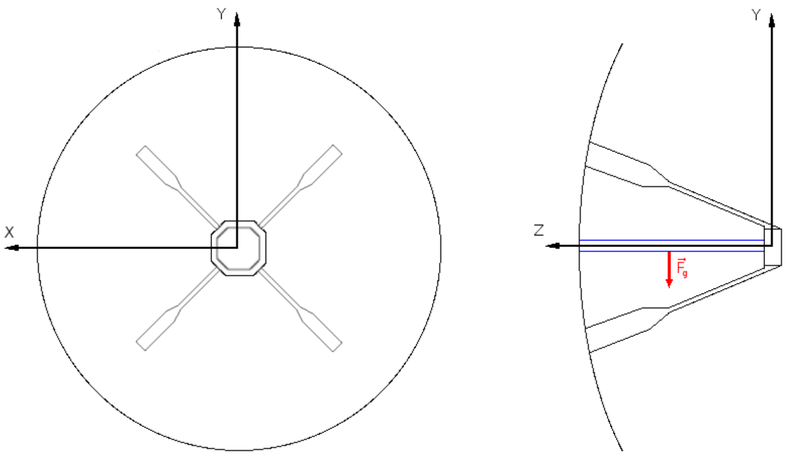

Figure 17: *Coordinate system used to model the subreflector equations. Gravity affecting an hypothetical rod (in blue) connecting the main and the secondary mirror. Telescope looking towards the horizon at 0 degrees elevation.*

Looking at Fig. 17, we realise that our coordinate system is fixed to the telescope, and so, independent of what the pointing position is. Accordingly, is the gravity field vector which varies with elevation:

$$\overrightarrow{g} = -gcosEl\widehat{y} + gsinEl\widehat{z} \tag{23}$$

And therefore, it is assumed that our subreflector model has to follow the same dependence. It is: a constant paramenter in x-axis, a *cosine* of elevation y-axis dependence, and *sine* of elevation in z-axis.